

Underexpression of *PpDXS1* gene decreased plant height and resulted in altered accumulation of phytohormones in Kentucky bluegrass

Lu Gan^{1,2*}, Yuehui Chao², Liebao Han², and Shuxia Yin^{2*}

¹ College of Animal Science and Technology, Yangzhou University, Yangzhou 225009, China P.R.

² College of Grassland Science, Beijing Forestry University, Beijing 100083, China P.R.

* Corresponding author, E-mail: ganlu2019@yzu.edu.cn; yinsx369@bjfu.edu.cn

Abstract

1-deoxy-D-xylulose-5-phosphate synthase (DXS) catalyzes the first and rate-limiting step of the plastidic 2-C-methyl-D-erythritol-4-phosphate (MEP) pathway which regulates the synthesis of terpenoids, such as gibberellins, abscisic acid, and chlorophyll. The objective of this study was to determine the functional role of *PpDXS1* in plant growth and development in Kentucky bluegrass (*Poa pratensis* L.). The *PpDXS1* gene has a 2139 bp open reading frame that encodes a polypeptide of 712 amino acids with a calculated molecular weight of 76.7 kDa. *PpDXS1* gene expression was the highest in leaves. Moreover, the *PpDXS1* promoter contained several hormone response elements and gene expression was induced by exogenous treatment with gibberellin, abscisic acid, jasmonate, and pathogen infection. Functional analysis indicated that underexpression of *PpDXS1* gene in *Poa pratensis* decreased plant height and endogenous gibberellin and indole acetic acid production, but promoted abscisic acid accumulation. Furthermore, transcriptome analysis and qRT-PCR results showed that the expression levels of related genes involved in the phytohormone biosynthesis and signal transduction were differentially regulated by *PpDXS1* in transgenic *Poa pratensis*. Overall, these results indicated that *PpDXS1* has strong effects on plant height and accumulation of phytohormones, and provided a preliminary understanding of molecular characterization, expression and function of *PpDXS1* in *Poa pratensis*.

Citation: Gan L, Chao Y, Han L, Yin S. 2021. Underexpression of *PpDXS1* gene decreased plant height and resulted in altered accumulation of phytohormones in Kentucky bluegrass. *Grass Research* 1: 9 <https://doi.org/10.48130/GR-2021-0009>

INTRODUCTION

Terpenoids constitute a large group of metabolites and have highly diverse structures and functions. Terpenoid primary metabolites, such as plastoquinone, phytosterol, chlorophyll, carotenoids, and phytohormones, participate in respiration, membrane fluidity, photosynthesis, and regulation of growth and development^[1–3]. Some secondary metabolites, such as phytoalexin, participate in allelopathic and plant-pathogen interactions^[4]. All terpenoids are derived from two common precursors, isopentenyl diphosphate (IPP) and dimethylallyl diphosphate (DMAPP), which are biosynthesized in plants through the cytosolic mevalonate (MVA) and plastidic methylerythritol phosphate (MEP) pathways^[5]. The MVA pathway is involved in synthesis of sesquiterpene, triterpene, and sterols, while the MEP pathway produces monoterpene, diterpene, and other secondary metabolites^[5]. Evidence suggests that there is metabolic flux between the two pathways via a metabolic network^[6,7], but normal levels of the end products are maintained in disrupted pathways by the respective regulation.

The first step of the MEP pathway is catalyzed by 1-deoxy-D-xylulose-5-phosphate (DXP) synthase (DXS) and produces DXP from glyceraldehyde-3-phosphate and pyruvate. As known, a series of enzymatic reactions was further presented in the MEP pathway (Fig. 1). The gene encoding DXS enzyme was first identified in *Escherichia coli* and DXS homologs were

subsequently found in model plants and crops, including *Arabidopsis*^[8], barrel clover^[9], tomato^[10], rice^[11], and maize^[12], suggesting that DXS genes are highly conserved in plants. Studies to date show that DXS enzyme is encoded by a small gene family. Multiple DXS genes have been found in *Medicago truncatula*^[9], *Oryza sativa*^[11], *Picea abies*^[13], *Zea mays*^[12], *Salvia miltiorrhiza*^[14], *Aquilaria sinensis*^[15], and *Artemisia annua*^[16], and two or three DXS genes in these plants cluster into three independent clades. It has been shown that DXS genes can also be divided into two types based on DXS function. DXS1 type is thought to be involved in primary metabolism (e.g. chlorophyll synthesis, photosynthetic processes), and mainly expressed in photosynthetic tissues^[9,17–19]. Unlike DXS1 genes in other plants, studies in *Aquilaria sinensis* have shown that *AsDXS1* is mainly expressed in the stems and were significantly induced by wound signals, indicating the involvement of *AsDXS1* in sesquiterpene formation^[15]. In addition, DXS1 gene also plays a role in carotenoid accumulation during fruit ripening in tomato and pepper^[10,20]. On the other hand, DXS2 type enzyme is thought to be involved in biotic or abiotic resistance defenses and metabolism of special secondary metabolites. For instance, the expression of DXS2 in barrel clover (*Medicago truncatula*) and maize (*Zea mays*) make different influences in the apocarotenoid accumulation during mycorrhization^[9,12]. The clade 3 of DXS gene, which is rarely identified in plants, often plays an interesting role in various plants. For example,

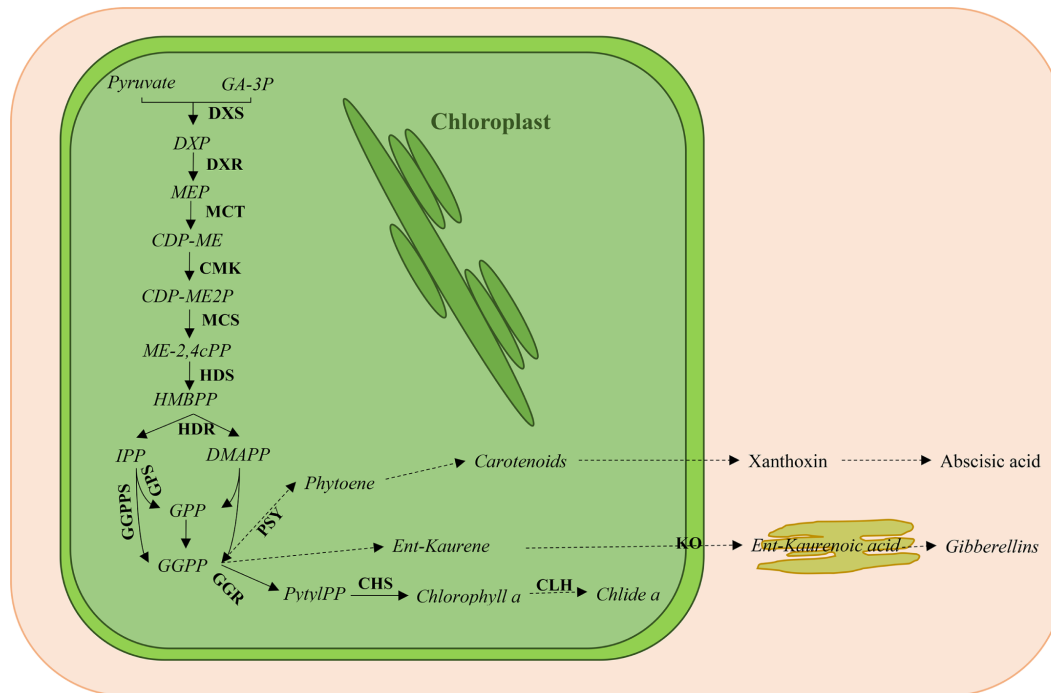


Fig. 1 Overview of the plastidic methyl erythritol phosphate (MEP) pathway for isoprenoid biosynthesis. GA-3P, glyceraldehyde-3-phosphate; DXS, 1-deoxy-D-xylulose-5-phosphate synthase; DXP, 1-deoxy-D-xylulose-5-phosphate; DXR, 1-deoxy-D-xylulose reductase; MEP, methylerythritol phosphate; MCT, MEP cytidyltransferase; CDP-ME, 4-(cytidine 5'-diphosphate)-2-C-methylerythritol; CMK, CDP-ME kinase; CDP-ME2P, 2-Phospho-4-(cytidine 5'-diphospho)-2-C-methylerythritol; MCS, 2-C-methylerythritol 2,4-cyclodiphosphate (ME-2,4cPP) synthase; HDS, 1-hydroxy-2-methyl-2-butenyl 4-diphosphate (HMBPP) synthase; HDR, HMBPP reductase; IPP, isopentenyl diphosphate; DMAPP, dimethylallyl diphosphate; GPPS, geranyl diphosphate (GPP) synthase; GGPPS, geranylgeranyl diphosphate (GGPP) synthase; PSY, phytoene synthase; GGR, geranylgeranyl reductase; PhytlPP, phytyl diphosphate; CHS, chlorophyll synthase; CLH, chlorophyllase; KO, ent-kaurene oxidase. Solid lines indicate a single enzymatic step, and dashed lines indicate several enzymatic steps.

DXS3 in rice has been suggested to also participate in defense responses^[21]. In the accumulation of terpenes and linalool in 'Jumeigui' grape, only the higher transcript abundance of *VvDXS3* showed significant correlation^[22].

Additionally, post-transcriptional and post-translational regulation are also important objectives of *DXS* functional mechanism research, as well as *DXS* gene expression and activity which are also regulated by external factors^[8]. For example, Mansouri et al. found that *DXS* enzymatic activity decreased after application of gibberellic acid^[23]. While *DXS* appear to have a universal function and evolutionary conservation, their functional action is species-specific. So, it is worth further exploring the metabolic regulation and movement for the isoprenoid product in plant growth and development.

While substantial progress has been made in understanding the function of the *DXS* in various plants (including model plants, crop and medicinal plants), little is known in the *Poaceae* family. There has been no research to date in the turfgrass field. Kentucky bluegrass, which belongs to the *Poaceae* family, is an important cool-season turfgrass in temperate and subarctic regions. Kentucky bluegrass has an aesthetic appearance and an excellent tolerance to low temperatures^[24], but requires frequent mowing to maintain turf quality^[25]. A preferred strategy is to use cultivars with shorter stature and good stress-resistance to reduce mowing frequency and improve quality. As previously reported, the MEP pathway and *DXS* genes play important roles in the

biosynthesis of various metabolites, such as gibberellin (GAs), abscisic acid (ABA), and in regulating plant growth and development^[7,26]. However, no *DXS* genes was isolated from Kentucky bluegrass, and little is known regarding the effects of *DXS* on growth and development in turfgrasses.

Previously, our work reported that *DXS1* homologous gene expression level is significantly lower in the dwarf mutant than in the wild-type^[27]. The dwarf mutant was obtained from F3 plants derived from 'Baron' seeds exposed to space environment on the satellite which usually results in abundant and non-directional mutations. Additionally, there are differences in leaf color, plant height and other traits between mutant and wild-type plants. Therefore, we studied the relationship between *DXS1* gene and plant growth, subsequently understanding the physiological differences between mutant and wild-type plants. In this study, we (a) isolated and characterized a *DXS1* gene from Kentucky bluegrass, (b) identified its regulatory effects on the biosynthesis and metabolism of various isoprenoids, and (c) used an underexpressing transgenic line to examine the functional role of *PpDXS1* in plant growth and development.

RESULTS

Isolation and analysis of *PpDXS1*

Three *DXS* homologous unigenes were selected from the *P. pratensis* transcriptome database (NCBI accession number: SRA315988) and then assembled for a fragment sequence for

putative *P. pratensis* DXS gene. RACE primers were designed against the candidate sequence and used to clone the putative DXS ORF frame from Kentucky bluegrass 'Baron' cultivar. An ORF of 2139 bp was produced and named *PpDXS1*. Sequence alignments revealed that *PpDXS1* amino acid sequence was very similar to DXS1 proteins from other plants (Supplemental Fig. S1a), including *Hordeum vulgare* (97% identity), *Aegilops tauschii* (97% identity), *Brachypodium distachyon* (95% identity), *Setaria italica* (90% identity), and *Oryza brachyantha* (90% identity).

PpDXS1 amino acid sequence and structure were examined further to elucidate functional features. The *PpDXS1* protein contained 712 amino acid residues and had a predicted molecular mass of 76.7 kDa and deduced isoelectric point of 6.5. Protein subcellular localization of *PpDXS1* was predicted in the chloroplast by the WoLF PSORT server, which was consistent with previous studies in various plants^[19,28]. Additional primary structure features are shown in Supplemental Fig. S1. The crystal structure of *PpDXS1* was not available in the SWISS-MODEL database. Available protein sequences were therefore used with the ExPasy server to deduce a 3D model for *PpDXS1*, with a model for *AtDXS* also constructed for comparison. Highly conserved functional residues in *PpDXS1* and *AtDXS* were predicted using the InterPro server. Residues 62–259 were highly conserved and formed a thiamine diphosphate binding pocket. Additional common domains important for biological function were also identified (Fig. 2). Differences between *AtDXS* and *PpDXS1* were observed from 648/654 residues onwards (Fig. 2; shown in red and yellow). Therefore, it is speculated whether the difference in DXS1 protein structure among different species will perform different functions in plants.

Phylogenetic analysis of DXS amino acid sequences among plants

PpDXS1 was shown to have a close relationship with *Aegilops tauschii*, *Brachypodium distachyon* and other *Poaceae* plants (Fig. 3). The phylogenetic tree grouped into three independent clades of DXS proteins conserved among plants. The first group referred to DXS1 proteins from a

variety of dicots and monocots. However, a DXS-like protein from *Arabidopsis* (*At3g21500*) also belongs to this group and its function is still unknown^[19,29]. The clade 2 proteins are mainly involved in secondary metabolism and includes *Oryza sativa* DXS2 together with representatives from woody plants (e.g. *Picea abies* and *Ginkgo biloba*)^[11,13,30]. Finally, the clade 3 proteins include *Arabidopsis* DXS3, rice DXS3, maize DXS3 and agarwood DXS3. As shown, the third branch is the distant phylogenetic DXS group. In this study, *PpDXS1* belonged to the DXS1 clade, but *PpDXS2* probably exists in Kentucky bluegrass because of its polyploidy. In rice and maize, two DXS1 proteins are also clustered into clade 1 and have been reported to participate in primary metabolism^[11,12], while *BdDXS1* in *Brachypodium distachyon* and *AetDXS1* protein in *Aegilops tauschii* had not been reported for functions. DXS1 protein not only participates in photosynthesis in most plants, but has also been shown to be involved in sesquiterpene metabolism and plant protection in agarwood (*Aquilaria sinensis*) and potato (*Solanum tuberosum* L.)^[15,18,31]. It is implied that DXS1 proteins among species perform conserved yet distinct functions. So, our findings in DXS1 would be beneficial to closely related *Poaceae* members associated with regulation of plant growth and development.

Isolation and analysis of the *PpDXS* upstream region

The 5' upstream region of *PpDXS1* gene (1,649 bp) were also isolated from Kentucky bluegrass (Supplemental Fig. S2). Cis-acting elements of the 5' upstream region were predicted using the PlantCARE and MAT-INSPECTOR databases. The predicted elements corresponded to light response, hormone metabolism, and stress defense regulation (Fig. 4). Relevant response elements included the ABRE element (ABA response), CGTCA-motif (related to MeJA response), GARE-motif (gibberellin response), box-W1 (fungal responsive element), G-box and L-box (involved in light responsiveness), and protein binding sites (HD-ZIP3, and MBS). The impacts of the different motifs and elements on inducible *PpDXS* expression and function in Kentucky bluegrass were examined further.



Fig. 2 ExPasy structure prediction models of *PpDXS* and *AtDXS*. Model images were generated using Chimera and conserved domains were analyzed using the InterPro server. Residues 62–259 (*PpDXS*) and 74–273 (*AtDXS*) represent the THDP-binding domain (green). Residues 387–552 (*PpDXS*) and 399–564 (*AtDXS*) represent the thansketolase_pyr_3 domain (blue). Residues 566–698 (*PpDXS*) and 578–701 (*AtDXS*) represent the thansketolase_C domain (pink). Differences between the *PpDXS* and *AtDXS* model are shown in red (*PpDXS*) and yellow (*AtDXS*).

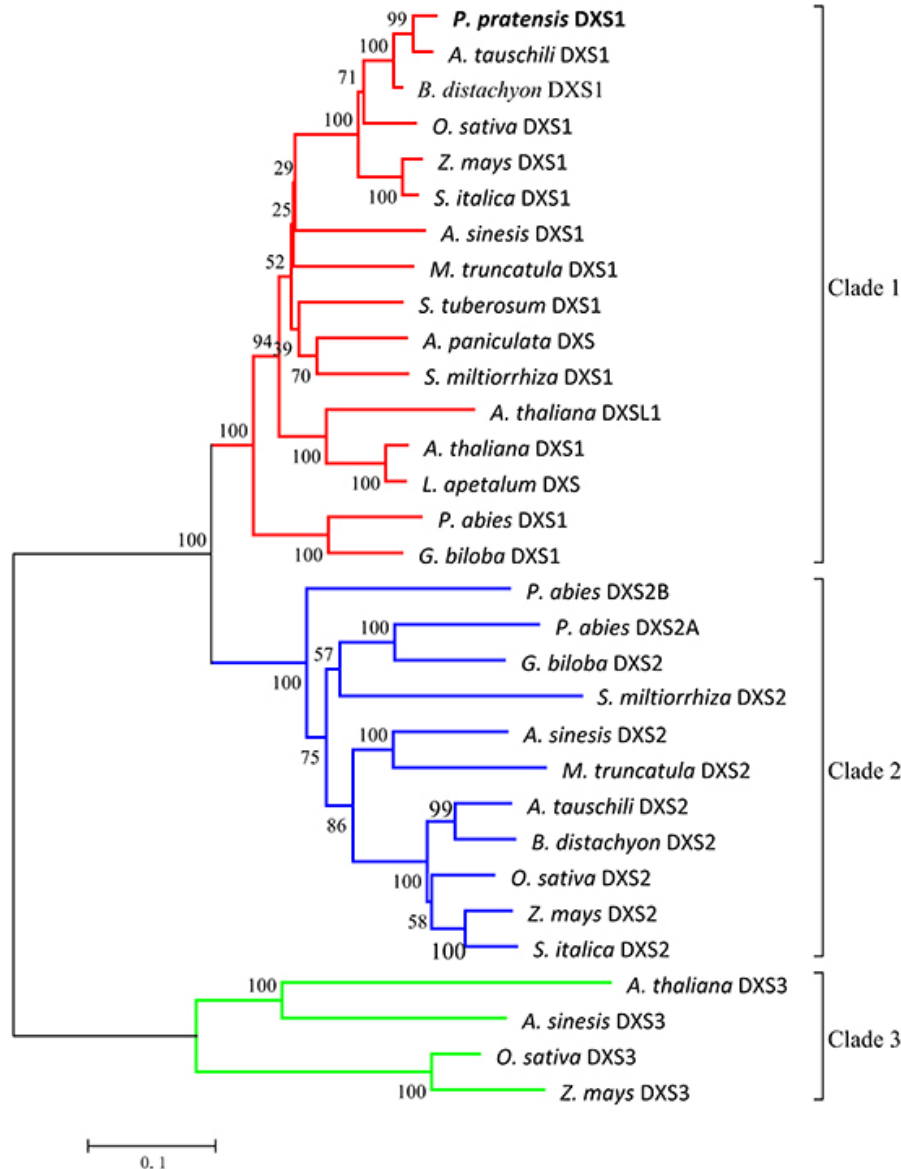


Fig. 3 Phylogenetic tree of plant DXS proteins. The tree was constructed with the neighbor-joining method and the JTT model using MEGA 5.0 software with 1,000 bootstrap values. The TAIR or GenBank accession numbers of DXS amino acid sequences used for phylogenetic analysis are as follows: *Arabidopsis thaliana* (DXS1 clade At4g15560, DXSL1 clade At3g21500, DXS3 clade At5g11380); *Oryza sativa* (DXS1 clade NP_00105524.1, DXS2 clade NP_001059086.1, DXS3 clade BAA83576.1); *Zea mays* (DXS1 clade NP_001157805.1, DXS2 clade NP_001295426.1, DXS3 clade HQ113384.1); *Aquilaria sinensis* (DXS1 clade AFU75321.1, DXS2 clade AHI62962.1, DXS3 clade AFU75320); *Andrographis paniculata* (DXS, AAP14353.1); *Lepidium apetalum* (DXS, KU314760.1); *Medicago truncatula* (DXS1 clade CAD22530.1, DXS2 clade CAN89181.1); *Picea abies* (DXS1 clade ABS50518.1, DXS2A clade ABS50519.1, DXS2B clade ABS50520.1); *Salvia miltiorrhiza* (DXS1 clade ACF21004.1, DXS2 clade ACQ66107.1); *Solanum tuberosum* (DXS1 clade NP_001275130.1); *Ginkgo biloba* (DXS1 clade AAS89341.1, DXS2 clade AAR95699.1); *Aegilops tauschili* (DXS1 clade XP_020161542.1, DXS2 clade XP_020164020.1); *Brachypodium distachyon* (DXS1 clade XP_003568467.1, DXS2 clade XP_003557443.1); *Setaria italica* (DXS1 clade XP_004962111.1, DXS2 clade XP_004955719.1). *Poa pratensis* (DXS1 clade MG257788).

Expression analysis of the *PpDXS1* in different tissues in *P. pratensis*

To gain insight into the expression pattern of *PpDXS1*, several tissues at a range of growth stages were examined in a quantitative real-time PCR experiment. As shown in Fig. 5, *PpDXS1* transcripts were detectable in different tissues (roots, leaf sheaths, and leaves), but accumulated predominantly in green tissues including young and mature leaves. The transcript abundance of *PpDXS1* was highest in mature plants, followed by young leaves. It is evidenced that the *PpDXS1*

gene belonged to *DXS1* type (consistent with phylogenetic analysis) and may be involved in photosynthesis. Additionally, the transcript level of *PpDXS1* was lower at the heading stage than in the developing leaves.

Regulation of different inducible factors on *PpDXS1* gene expression in *P. pratensis*

DXS is the rate-limiting enzyme in the MEP pathway, which is involved in the formation of diverse terpenoids, including important phytohormones for plant growth. Results shown in

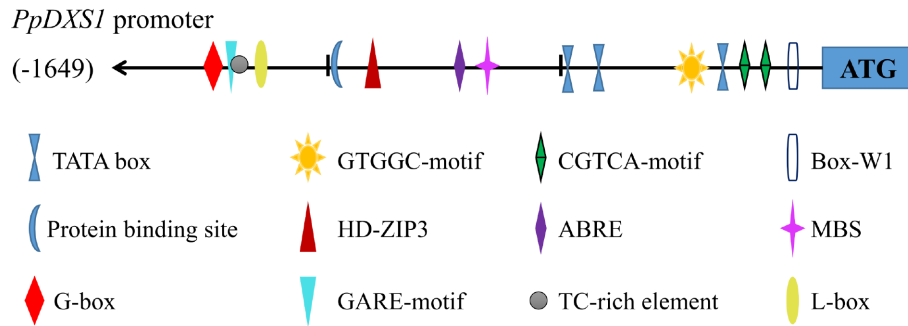


Fig. 4 *PpDXS1* promoter from *P. pratensis*. Putative cis elements are labeled as shown, Element positions are shown proportional to the full length of the promoter.

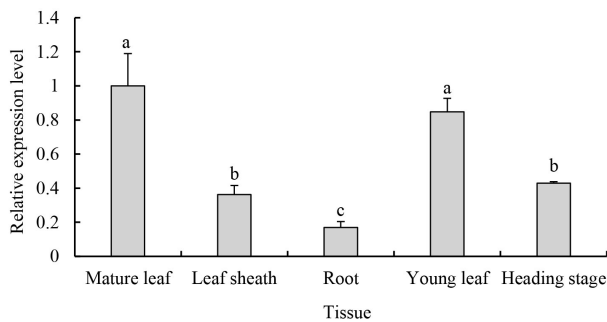


Fig. 5 *PpDXS1* expression analysis in *P. pratensis*. Quantitative RT-PCR analysis of *PpDXS1* gene expression. Fully expanded leaves (named as mature leaf), leaf sheaths and roots at vigorous growth stage were used for gene organ/tissue-specific expression analysis. For the time-series gene expression analysis, young leaves at early growth stage (named as young leaf), mature leaves at vigorous growth stage (similarly named as mature leaf), and old leaves at heading stage (named heading stage) were used. All qRT-PCR reactions were performed from triplicate biological samples. The $2^{-\Delta\Delta Ct}$ method was used to calculate the fold expression relative to the control (mature leaf). Means of three replicates \pm standard error is shown. Bars superscripted with different letters are significantly different at $p < 0.05$.

Fig. 4 show that the response elements and motif of ABA (ABRE), JA (CGTCA-motif), GA(GARE-motif), and fungal (box-W1) were identified in the *PpDXS1* promoter sequence. Therefore, we examined the effects of exogenous factors on *PpDXS1* expression in *P. pratensis*. Plants were exposed to foliar applications of GA₃, ABA, JA, or pathogen inoculation, and the relative expression level of *PpDXS1* were determined in the leaves collected 0, 3, 6, and 12 h after treatment (Fig. 6).

As shown in Fig. 6, GA₃ treatment had a positive effect on *PpDXS1* gene expression and the level peaked 3 h after application. Meanwhile, increased transcript level of *PpDXS1* 6 h and 12 h after ABA treatment was observed, while the fold change of ABA regulation has a lower value, compared to GA₃ treatment. It is predicted that exogenous ABA have a slight impact on *PpDXS1* gene expression, compared with GA₃ treatment. After JA treatment, *PpDXS1* expression was induced and peaked at the 3h-point (5.6-fold). A similar response was seen after pathogen inoculation. Gene expression was stimulated, and peaked at 6 h after inoculation (4.2-fold). On the other hand, it is indicated that the inductive effect of exogenous JA was faster than the pathogen infection for *P. pratensis*.

Effect of *PpDXS1* underexpression on plant height, chlorophyll and hormone content in *P. pratensis*

To test the role of *PpDXS1* in regulating the terpenoid biosynthetic pathway in *P. pratensis*, three transgenic lines with antisense expression of *PpDXS1* gene and empty vector (CK) of Kentucky bluegrass were obtained by screening and identification. In order to further determine the positive plants, western blot analysis was carried out for the extracted protein from transgenic plants and the CK plant (Fig. 7a). The result showed that the *PpDXS1* protein level (the band of 76 kDa) decreased in the transgenic anti*DXS1*-56/-102 lines, except the anti*DXS1*-101 strain which was not used for further research (Fig. 7a and supplemental Table S1). It is indicated that *DXS1* protein accumulation could be decreased by antisense expression of the *PpDXS1* gene. It should be noted here that there is another band below the target band (i.e. 74 kDa) in Fig. 7a, which indicated that the second band could be the *DXS2* protein of Kentucky bluegrass as the specificity of the *PpDXS1* polyclonal antibody in this study was not very high.

Additionally, transgenic lines displayed the phenotype of reduced plant height. As shown in Fig. 7b and c, Plant height was reduced in transgenic lines by approximately 40% relative to CK. For chlorophyll, the total pigment content of transgenic anti*DXS1*-56 is significantly higher than that of CK, but the difference between anti*DXS1*-102 and CK is not significant (Fig. 7c).

Differences in phytohormones content between transgenic lines and the control plant were also analyzed. All *DXS1*-transformed lines showed decreased GAs and IAA content compared with that of the control (Fig. 7d). By contrast, the accumulation of ABA in the transgenic plant were increased. There are different accumulation among GAs, IAA and ABA content in transgenic *P. pratensis*, which may be related to the various regulation of *DXS1* gene. In general, it is illustrated that *PpDXS1* is an important gene in the regulation of phytohormone and chlorophyll accumulation.

Underexpression of *PpDXS1* gene regulated the differential gene expression involved in hormone anabolism in transgenic *P. pratensis*

To study the effects of *PpDXS1* underexpression on plant growth and development, RNA-seq analysis was used to compare transcriptional level in CK and an underexpressing antisense line (anti*DXS1*-102). Differential gene expression analysis revealed a total of 3,800 genes whose expression

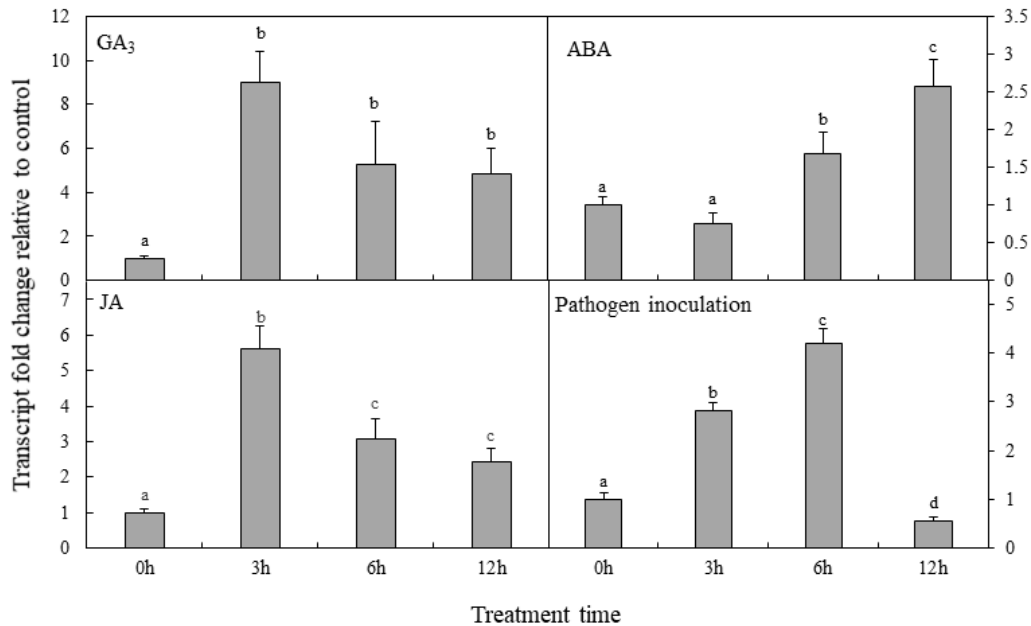


Fig. 6 Analysis of *PpDXS1* expression after exogenous phytohormone treatment or pathogen inoculation in *P. pratensis*. Quantitative real-time PCR analysis of relative *PpDXS1* expression after foliar exposure to gibberellic acid (GA₃), abscisic acid (ABA), jasmonate (JA), and pathogen inoculation. All qRT-PCR reactions were performed from triplicate biological samples. The $2^{-\Delta\Delta C_t}$ method was used to calculate the fold expression relative to the control (0h-point). Mean of three replicates \pm standard error is shown. Bars superscripted with different letters are significantly different at $p < 0.05$.

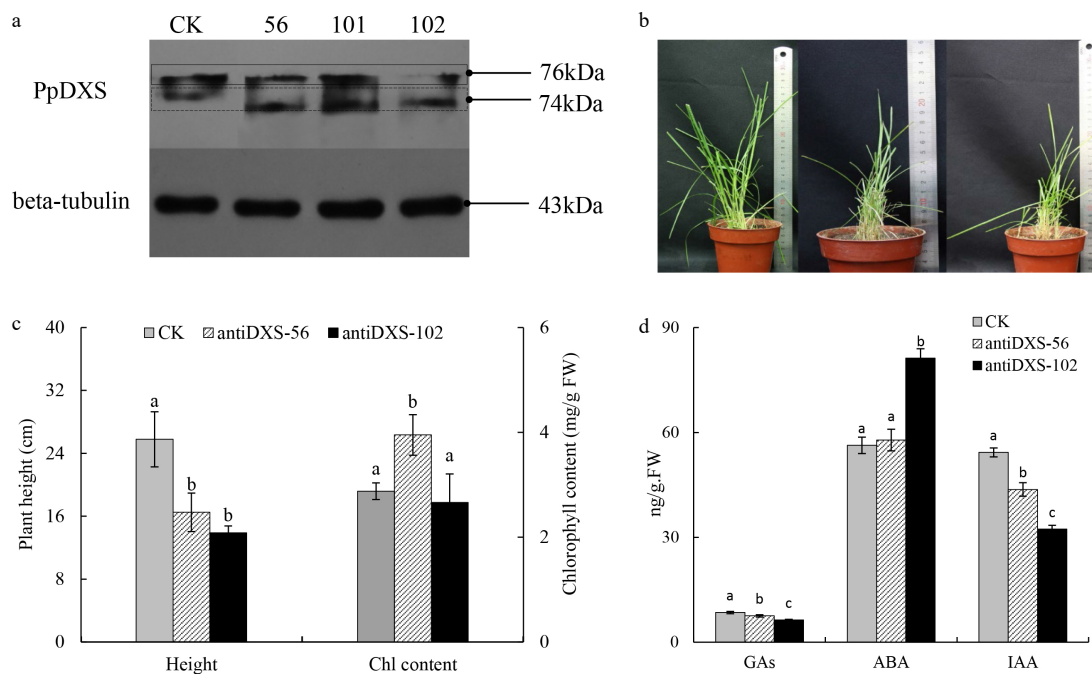


Fig. 7 Comparison of CK and transgenic lines underexpressing *PpDXS1* in *Poa pratensis*. (a) Western analysis of PpDXS1 protein levels in mature leaves of CK and antiDXS1-56, -101, and -102. (b) The photos of CK, antiDXS1-56 and antiDXS1-102 transgenic plants (left to right). (c) Plant height and total chlorophyll content of CK, antiDXS1-56 and antiDXS1-102 transgenic plants. Bars superscripted with different letters are significantly different at $p < 0.05$. (d) Phytohormone content of CK, antiDXS1-56 and antiDXS1-102 transgenic plants. Means of three replicates \pm standard error is shown. The data were subjected to ANOVA test to determine the LSD between CK (control) and transgenic lines (antiDXS1-56 and antiDXS1-102) at $p < 0.05$.

significantly differed (\log_2 fold change ≥ 1 and q value < 0.005) between antiDXS1-102 and CK, 1845 and 1955 of which were up- and down-regulated in antiDXS1-102, respectively

(Supplemental Fig. S3a). The differentially expressed genes (DEGs) were involved in diverse biological processes such as terpene synthase activity, protein kinase activity, and

metabolic processes (Supplemental Fig. S3b, c). On the basis of enrichment analysis and related keywords of KEGG pathway and GO terms, some DEGs between CK and antiDXS1-102 line were summarized in Fig. 8a. Firstly, one DXS unigene was down-regulated in the transgenic line, while other related isoprenoid biosynthetic genes (e.g. FPS and SPS) are up-regulated. Secondly, the expression of genes related to auxin biosynthesis and signal transduction were affected, for example the transcripts encoding auxin responsive factor 9 (ARF9) was down-regulated. Similarly, the GA20ox2 gene involved in gibberellin biosynthesis was down-regulated in the transgenic line. Conversely, ABA biosynthetic genes were enriched in the transformed line compared to CK, such as phytoene synthase (PSY) gene and 9-cis-epoxycarotenoid dio-

xxygenase 1 (NCED1) gene. Finally, in the pathway of chlorophyll biosynthesis and metabolism, the expression level of geranylgeranyl reductase (GGR) genes and chlorophyllide a oxygenase (CAO) genes that promoted chlorophyll a (or side chain) synthesis were increased. The CLH gene which directs chlorophyll degradation were down-regulated in the antiDXS1-102 line, while the increase of chlorophyll content in the antiDXS1-102 line was not significant. These observations were consistent with the above result of phenotype and physiological characteristics in the transgenic line, which indicate that PpDXS1 directly influences the production of physiological metabolites, particularly those producing GA, IAA, and ABA at the end of the MEP pathway.

To verify the RNA-seq data and further investigate the

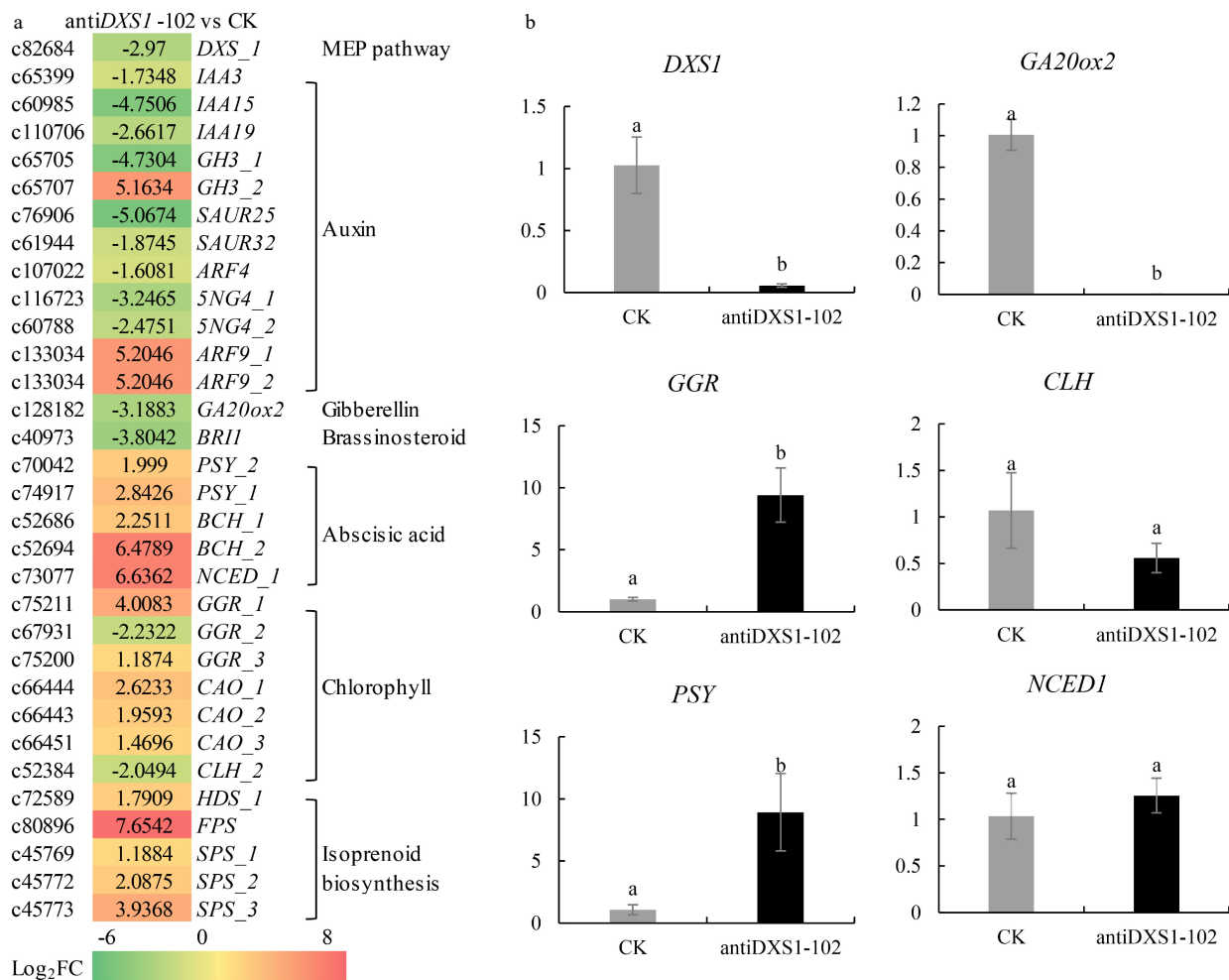


Fig. 8 Differential expression analysis of related genes in CK and antiDXS1-102. (a) Heatmaps of differentially expressed genes (DEGs). *DXS*, 1-deoxy-D-xylulose-5-phosphate synthase; *IAA3/15/19*, auxin-responsive protein 3/15/19; *GH3*, indole-3-acetic acid-amido synthetase *GH3* gene family; *SAUR25/32*, auxin-responsive SAUR protein family; *ARF9*, auxin responsive factor 9; *GA20ox2*, gibberellin 20 oxidase 1; *BRI1*, brassinosteroid-insensitive 1; *PSY*, phytoene synthase; *BCH*, beta-carotene hydroxylase; *NCED1*, 9-cis epoxycarotenoid dioxygenase 1; *GGR*, geranylgeranyl reductase; *CLH*, chlorophyllase; *CAO*, chlorophyllide a oxygenase; *HDS*, 1-hydroxy-2-methyl-2-butenyl 4-diphosphate (HMBPP) synthase; *FPS*, farnesyl diphosphate synthase; *SPS*, solanesyl-diphosphate synthase. Upregulation and downregulation in antiDXS1-102 compared to CK are shown using a color scale for log₂ (antiDXS1-102/WT ratio) values. On the left side of the color block is the Unigene ID from the transcriptome database, and on the right side is the gene annotation in the database. (b) qRT-PCR results of selected six DEGs. The transformed line of empty vector (CK) is the control and the value is one. The 2^{-ΔΔCT} method was used to calculate the value of fold change compared to the control (CK, the transformed line of empty vector). All qRT-PCR reactions were performed from triplicate biological samples. Mean of three replicates ± 1 standard error is shown. Bars with superscript letters are significantly different at p < 0.05.

above DEGs, quantitative real-time PCR assays were performed for selected genes with significantly different transcription levels between CK and antiDXS1-102, namely *DXS1*, *GA20ox1*, *GGR*, *CLH*, *PSY1*, and *NCED1*. Expression of *DXS1* and *GA20ox1* was lower in antiDXS1-102 than in CK (Fig. 8b), indicating that antisense expression of *PpDXS1* impacted the lower transcription of genes involved in GA synthesis. Meanwhile, *GGR* gene, involved in the biosynthesis of phytyl diphosphate and chlorophyll a, exhibited higher expression in the antiDXS1-102 line. Higher expression of *PSY* was seen in antiDXS1-102 than in CK, which corresponded with the RNA-seq results.

DISCUSSION

The MEP pathway, also known as the non-mevalonate route, was identified as an alternative terpenoid biosynthesis pathway in Eubacteria and higher plants^[32]. There has been substantial progress in the identification of *DXS* genes, the first rate-limiting enzyme of the MEP pathway^[18,33,34]. Although *DXS1* function has been studied in many plants, little is known about the *Poaceae* family and in particular turfgrasses. In this study, a 2139 bp ORF and the upstream region of the *PpDXS1* gene were isolated from *P. pratensis*. To our knowledge, this is the first report of *DXS1* isolation from turfgrass, and the first study to examine metabolic regulation of isoprenoid biosynthesis in this plant.

DXS1 has also been annotated in *Aegilops tauschii* (*AetDXS1*) and *Brachypodium distachyon* (*BdDXS1*) with its nucleotide sequence released in NCBI, which show high similarity to *PpDXS1* as found in this study, however, the physiological functions of *AetDXS1* and *BdDXS1* have not been previously reported. In this study, it was found that *PpDXS1* possesses a conserved motif with a thiamine diphosphate binding site and transketolase motif. Bioinformatic subcellular localization prediction suggested that *PpDXS1* is located in the chloroplast. In the present study, the *PpDXS1* gene expression occurred in the leaves, leaf sheath, and root with the highest transcription level in leaves (Fig. 5). In *Medicago truncatula* and tobacco plants, *DXS1* gene was also relatively higher in leaves and stems than in the roots^[9,35]. As shown in the results of the phylogenetic tree and expression assay in different tissues (Fig. 3 & 5), it is indicated that *PpDXS1* gene is probably in clade 1 of the *DXS* gene family, and is mainly expressed in leaves. Previous studies also suggest that *DXS1* type are responsible for the primary metabolism, including chlorophyll biosynthesis and photosynthetic process, and mainly performed the function in leaves^[12,36]. Additionally, Lois et al. reported that *DXS1* is probably involved in fruit ripening and sesquiterpene formation^[10]. However, in the recent report by García et al., it showed that *DXS1* gene plays a key role in plant development and survival at the early growth stage besides being related to fruit carotenoid synthesis^[37]. Therefore, it is indicated that *DXS1* perform conserved but species-specific function, and it is important to explore the concrete roles of *DXS* isoforms in the regulation of plant growth and development.

On the basis of prediction analysis on the 5' upstream region which often contains binding sites of regulatory factors, *PpDXS1* gene expression increased after treatment

with GA₃ and ABA. Similarly, Yang et al. reported that ABA treatment upregulated *SmDXS* transcription in *Salvia miltiorrhiza* hairy roots^[38]. Interestingly, the fold change of GA treatment were generally higher than those of other induced treatments, which indicated that GA₃ had more effect on *PpDXS1* expression than ABA in *P. pratensis*. Also, plants produce secondary metabolites to adapt to unfavorable conditions, such as pathogen attack. JA and fungal infection act as signals to induce secondary metabolite biosynthesis by elevating expression of related genes. For example, *StDXS1* transcript levels were lower in *Solanum tuberosum* with symptoms of late blight (caused by the oomycete *Phytophthora infestans*), but expression was induced up to 12 h post-infection^[33]. Similarly, exogenous JA treatment stimulated the *GrDXS* expression in rose-scented geranium^[20]. In our study, *PpDXS1* transcript expression in leaves after JA treatment was highest at the 3h-point, increasing up to 6 h after pathogen inoculation. It is indicated that the pathogen infection has longer inductive effect of the expression of *PpDXS1* compared with the JA treatment. Although these changes are only observed in the leaves, it can not be ignored that the low level of *PpDXS1* gene expression is correlated with the pathogen inoculation and the accumulation of phytoalexin^[21].

DXS, as the rate-limiting enzyme of the MEP pathway, regulates the flux of the plant MEP pathway but how does it affect the biosynthesis of downstream terpenoids? The genetic transformation experiment described in the study was designed to evaluate the effects on plant growth and isoprenoid abundance. In this work, GAs and IAA levels were decreased, but higher accumulation of ABA occurred in the underexpression mutant compared to the CK plants of Kentucky bluegrass. In Arabidopsis, plants with *DXS* either overexpressed or suppressed different levels of the final isoprenoid products^[39]. In brief, the total chlorophyll and ABA contents of *DXS*-suppressed plants were significantly lower than those of the control plants, but the expression of *GA4* gene was up-regulated, and the overexpressed plants were the opposite. However, the GA content showed a higher level in Arabidopsis overexpressing the *DXS1* gene from *Morus notabilis*^[40]. Also, it is found that overexpression of *DXS1* from potato (*Solanum tuberosum*) resulted in a higher accumulation of chlorophyll and decreased ABA and GA₄ content in the transgenic Arabidopsis lines compared to control plants^[37]. Although various research of homologous or heterologous expression found that overexpression or underexpression of *DXS1* was linked to the same changes in isoprenoid levels^[20], it was not clear whether lower expression of *DXS* necessarily led to decreased production of all isoprenoid end products, which merited further investigation.

Aside from the measured changes in phytohormones content in this work, the significant decrease was observed in plant height of the antiDXS1-102 mutant compared to CK. These differences are likely due, in part, to observed changes in IAA and GA levels as changes in these hormones result in dwarf phenotype (Fig. 7d). Although *DXS* is the first rate-limiting enzyme in the MEP pathway, additional limiting and regulatory enzymes or genes also play indispensable roles in regulation of downstream terpenoids. For example, geranylgeranyl diphosphate synthase can also control the

flow of intermediates^[41]. So, to further identify the regulatory and control points of *DXS1* in the MEP pathway, RNA-seq was used to examine the expression of key MEP and related isoprenoid biosynthetic pathway genes in CK and anti*DXS1*-102 plants, to determine the effects of lowered *PpDXS1* levels on isoprenoid synthesis. DEG analysis revealed that genes involved in GA and IAA biosynthesis and signal transduction pathways were downregulated in the anti*DXS1*-102 mutant compared to CK, which is consistent with the GA and IAA content. The anti*DXS1*-102 plant exhibited enhanced expression of ABA biosynthetic genes, again consistent with the ABA content. The state of the MEP pathway or intermediates were assumed to be in equilibrium with these decreased or increased downstream terpenoids. On the other hand, the overexpression or suppression of *PpDXS1* gene may influence the content of downstream isoprenoids, but each of these post-IPP biosynthetic pathways may have its own set of rate-limiting and regulatory steps^[5].

CONCLUSIONS

In the present study, functional analysis of *DXS1* in *P. pratensis* revealed that underexpression of *PpDXS1* on the MEP pathway have different impacts on terpenoid biosynthesis and physiology, including decreased plant height, endogenous GAs and IAA production, but promoted ABA accumulation, as well as the expression levels of related genes. This work provides not only important guidance to further study the role of *DXS1* in response to environmental stresses in turfgrass, but also an addition to the knowledge of *DXS1* enzyme in plants in general and *Poa pratensis* in particular.

MATERIALS AND METHODS

Plant materials and treatments

Kentucky bluegrass cultivar ‘Baron’ was used as wild type (WT). WT plants were grown in soil-sand-perlite (1:1:1, v/v) in SC-10 single-cell containers (12 cm diameter × 10 cm depth) at 25 °C with 14/10 h day/night photoperiod. In the WT growth process, young leaves at early growth stage, mature leaves at vigorous growth stage, and old leaves at heading stage were used for gene expression analysis of the time-series sample. In addition, fully expanded leaves, leaf sheaths and roots at vigorous growth stage were also used for gene organ/tissue-specific expression analysis. Plants were also

foliar sprayed with 30 mg/L gibberellic acid (GA₃), 10 mg/L abscisic acid (ABA), 535 mg/L jasmonate (JA), and a spore suspension of *Puccinia graminis*^[42]. The leaf samples were collected 3, 6, and 12 h after treatment and used for gene expression analysis.

Cloning the *PpDXS1* sequence of ORF and promoter region

Candidate nucleotide sequences of *DXS* unigenes from relatives of *P. pratensis* were used in Blastn searches of *P. pratensis* transcriptome sequences (NCBI accession number: SRA315988). Three candidate *DXS* unigenes were assembled and specific primers were designed to amplify the middle fragment. Then, specific primers (Table 1) for amplification of 5’ and 3’ fragments using a SMART RACE cDNA Amplification Kit (Clontech, USA). Fragments were amplified and 10 clones of full ORF sequence were confirmed by sequencing and blast. Finally, *PpDXS1* gene ORF sequence of one consistent clone are deposited in GenBank (accession numbers: MG257788).

Genomic DNA was extracted from WT leaves using a modified CTAB method. To clone the promoter region of *PpDXS*, high-efficiency thermal asymmetric interlaced PCR were performed using degenerate primers and specific nested-primers (Table 1, Supplemental Table S2) designed against the *PpDXS* ORF sequence. Amplified fragments produced by the nested PCR were cloned and then sequenced. Sequences (shown in Supplemental Fig. S2) that extended upstream of *PpDXS* were isolated and used for the further analysis. The 5’ upstream sequence was analyzed for putative cis-acting regulatory elements using the Plant CARE database.

Bioinformatics analysis of *PpDXS1*

DXS1 protein sequences were collected using the BLASTp program and were aligned using the ClustalW program (<http://www.ddbj.nig.ac.jp>) with standard parameters. The physical and chemical characteristics of the amino acid sequence were conducted in ProtParam program (<http://web.expasy.org/protparam>) and the subcellular localization were analyzed by TargetP 1.1 Server. The phylogenetic tree was generated by the neighbor-joining method on the MEGA5 software and bootstrap values were obtained from 1,000 replicates^[43]. Signal peptide and transmembrane topological structures were predicted by SignalP (<http://www.cbs.dtu.dk/services/SignalP>) and TMHMM 2.0 server (<http://www.cbs.dtu.dk/services/TMHMM>). Crystal structure of *PpDXS* and *AtDXS* were modeled using the ExPasy server and conserved protein domains were analyzed by searching the deduced

Table 1. Nucleotide sequences of gene-specific primers

Primer name	Sequence (5’-3’)	Description
3’-GSP	CGACGACCTCATCACCATCCTCCG	3’-RACE primer
5’-GSP	GTCTTGGTGCCCTTGACCTCCCG	5’-RACE-out-primer
5’-NEST	TCCGCCTATTTGCTTCGCACTCC	5’-RACE-in-primer
DXS-F	ATGGCGCTCTCGACGACGTTCT	ORF-F
DXS-R	CTAAACATTCTGCACCGTCATG	ORF-R
antiDXS-F(BstEII)	GGGTNACCATGGCGCTCTCGACGACGTTCT	Primers for vector construction
antiDXS-R(BglII)	GAAGATCTAACATTCTGCACCGTCATG	
SP1	CCGTCGGTCTGCCGCATCGTC	Primer for promoter amplification
SP2	TCGCTTGTCTGAGGGGTGTTG	
SP3	TGAGGGACAGGTTCTTCATGTGGA	

amino acid sequences against the NCBI Conserved Domain Database (CDD, <http://www.ncbi.nlm.nih.gov/Structure/cdd/wrpsb.cgi>). The subcellular localization was predicted using the WoLF PSORT server.

Relative expression analysis

Total RNA from root, leaf sheath and leaf were obtained with TRIzol reagent kit (Invitrogen, USA) using 100–500 mg tissue homogenized in liquid nitrogen. Its quantity and purity were assessed using the NanoDrop 2000 (Thermo, USA) and reverse transcriptional reaction was carried out with 0.5 µg total RNA using PrimeScript™ RT reagent Kit (Perfect Real Time) (Takara, Japan) according to the supplier's instruction.

Quantitative real-time PCR was carried out using a SYBR Green assay (Takara, Dalian, China) on a Bio-Rad CFX96 System (Roche, USA). Each 25 µL assay contained 12.5 µL SYBR Premix Ex Taq, 2 µL cDNA and 100 nM of each primer (Supplemental Table S2). For exogenous application, the relative mRNA abundance was calculated by using the comparative C_T method ($2^{-\Delta\Delta C_T}$) and normalization to 18S gene. The analysis included three biological replicates and three technical replicates for each sample. The data were statistically analyzed via the SPSS21.0 software, and subjected to one-way analysis of variance (ANOVA) to determine the least significant difference (LSD) among the treatments at $p < 0.05$.

Genetic transformation and regeneration of Kentucky bluegrass

Antisense oligonucleotides have been used for more than a decade to downregulate gene expression^[44]. So, in the study, an RNA antisense-expressing cassette targeting the *PpDXS1* gene was placed under the control of the CaMV 35S promoter and NOS terminator in the pCAMBIA1301 vector. The *PpDXS1* gene was amplified from a pGEMT-easy plasmid clone using gene-specific full-length primers that incorporated *Bgl*III and *Bst*EII restriction sites in the forward and reverse primers, respectively (Table 1). After amplification and restriction digestion, the *PpDXS1* gene was inserted into the entry plasmid pCAMBIA1301 to form recombinant plasmid pCAMBIA1301-antiDXS (Supplemental Fig. S4).

Embryogenic calli (approximately 100 small pieces of callus) were placed as a 2.5 cm diameter monolayer in a 5.0 cm Petri dish containing subculture medium (MS basal medium plus 30 g/L sucrose, 1 mg/L 2,4-D, 0.5 mg/L 6-BA, and 0.2 M mannitol) for 4–8 h of osmotic treatment prior to bombardment. Gold particles (0.6 µm, Bio-Rad, CA) were DNA-coated essentially as described by Ha et al.^[45]. The bombardment mixture contained 0.6 mg gold particles and 1 µg plasmid DNA per shot. Bombardment was carried out using a Biolistic PDS-1000/He Particle Delivery System (Bio-Rad, Supplemental Fig. S5) with a target distance of 6 cm. Bombarded calli were incubated on subculture medium overnight.

Callus bombarded with pCAMBIA1301-antiDXS1 and pCAMBIA1301 empty vector were incubated in subculture medium for 7 d and then transferred to selected regeneration medium containing 100 mg/L hygromycin and a certain amount of 6-BA and KT. After two selection rounds with 100 mg/L hygromycin under dark conditions, hygromycin resistance callus was transferred to regeneration medium

supplemented with 50 mg/L hygromycin and incubated under a 16/8-h (light/dark) photoperiod. Fully recovered plantlets were transferred to containers for further root development and, finally, green plants were transferred to soil in a greenhouse. Transformed plants of pCAMBIA1301-antiDXS1 were identified in T0 plants by PCR with three pairs of specific primers for the hygromycin gene (Hyg-F/R, 517 bp), 35S promoter regions (35S-F/R, 195 bp) and compound primers (35S-F and antiDXS1-F), see details in Supplemental Table S2. And the transformed plants of empty vector (used as controls, namely CK) were identified by two pairs of primers of hygromycin gene and 35S promoter regions.

Protein extraction and western blot analysis

Total plant protein extracts were obtained from 50–100 mg of fresh tissue. Samples were ground in liquid nitrogen, suspended in 500–1,000 µL ice-cold RIPA buffer supplemented with 1 mM PMSF, and ultrasonicated. Resuspended samples were then centrifuged at 12,000 rpm for 10 min at 4 °C, and then the supernatant was recovered and re-centrifuged. Supernatant protein concentration was determined using the bicinchoninic acid (BCA) method. Proteins were separated using SDS-PAGE and then electrotransferred to polyvinylidene fluoride membranes (PALL, America). Membranes were incubated overnight at 4°C with primary antibody (diluted 1:500) then with horseradish peroxidase-conjugated secondary antibody (diluted 1:5,000) for 2 h at room temperature. The objective protein is a polyclonal antibody on the basis of designed immunogen fragments according to the predicted DXS protein sequence and synthesized by Abmart (Shanghai, China). Imaging and quantification were performed using Quantity One (Bio-Rad).

Analysis of plant height, endogenous hormone and chlorophyll content in transformed plants

Firstly, plant height of one CK and two antiDXS1-transformed lines was recorded and five replications were set in each pot. Then, fresh samples comprising the terminal bud and young leaves (0.3–1 g) from plants at the same stage of development were collected and used to determine endogenous hormone content. Levels of total GAs, ABA, IAA, and JA were determined using the ELISA method according to the manufacturer's protocol (supplied by the Crop Chemical Control Laboratory at China Agricultural University). Chlorophyll was extracted by soaking 50 mg of fresh leaves in 8 mL acetone (95%, v/v) for 72 h in the dark, followed by spectrophotometric quantification at 470, 645, and 663 nm (Beckman, CA, USA). Total chlorophyll content was calculated using the Arnon method^[46]. These data were statistically analyzed via the SPSS21.0 software, and subjected to one-way analysis of variance (ANOVA) to determine the least significant difference (LSD) between CK and antiDXS1 transgenic plants at $p < 0.05$.

Transcriptional expression analysis by RNA-sequencing

Kentucky bluegrass leaf blades were collected from the control (CK) and transformed plant of target gene (antiDXS1-102) and used for sequencing. Total mRNA was extracted using TRIzol Reagent (Invitrogen, USA) according to the manufacturer's instructions, and cDNA library construction

and normalization were performed as described previously^[47]. Total RNA samples were sequenced using the Illumina HiSeq platform. Cleaned and qualified reads were assembled *de novo* using Trinity software, as described previously^[48], and mapped to reference transcriptome libraries using RSEM (v 0.7) alignment. Read counts of transcripts with a reciprocal match to the reference transcriptome were extracted and calculated using FPKM (expected number of Fragments per Kilobase of transcript sequence per Million base pairs sequenced) values for gene expression analysis. The matrix of read counts was used with the DESeq R statistical package to identify transcripts with significant expression differences between antiDXS-102 and CK (FDR < 0.05). Log₂ (FPKM-antiDXS-102/FPKM-CK ratio) values were shown in heatmaps representing expression profiles of DEGs.

ACKNOWLEDGMENTS

All authors gratefully acknowledge the Forestry Central Laboratory of Beijing Forestry University for providing the research facilities. This study was supported by the National Natural Science Foundation of China (No. 31302016).

Conflict of interest

The authors declare that they have no conflict of interest.

Supplementary Information accompanies this paper at (<http://www.maxapress.com/article/doi/10.48130/GR-2021-0009>)

Dates

Received 26 March 2021; Accepted 22 September 2021; Published online 19 October 2021

REFERENCES

- Bach TJ. 1995. Some new aspects of isoprenoid biosynthesis in plants – a review. *Lipids* 30:191–202
- Disch A, Hemmerlin A, Bach TJ, Rohmer M. 1998. Mevalonate-derived isopentenyl diphosphate is the biosynthetic precursor of ubiquinone prenyl side chain in tobacco BY-2 cells. *Biochemical Journal* 331:615–21
- Rodríguez-Concepción M, Boronat A. 2015. Breaking new ground in the regulation of the early steps of plant isoprenoid biosynthesis. *Current Opinion in Plant Biology* 25:17–22
- Baker FC, Brooks CJW. 1976. Biosynthesis of the sesquiterpenoid, capsidiol, in sweet pepper fruits inoculated with fungal spores. *Phytochemistry* 15:689–94
- Vranová E, Coman D, Gruissem W. 2012. Structure and dynamics of the isoprenoid pathway network. *Mol Plant* 5:318–33
- Ratcliffe RG, Shachar-Hill Y. 2006. Measuring multiple fluxes through plant metabolic networks. *The Plant Journal* 45:490–511
- Vranová E, Coman D, Gruissem W. 2013. Network analysis of the MVA and MEP pathways for isoprenoid synthesis. *Annual Review of Plant Biology* 64:665–700
- Estévez JM, Cantero A, Romero C, Kawaide H, Jiménez LF, et al. 2000. Analysis of the expression of *CLA1*, a gene that encodes the 1-deoxyxylulose 5-phosphate synthase of the 2-C-methyl-D-erythritol-4-phosphate pathway in *Arabidopsis*. *Plant physiology* 124:95–104
- Walter MH, Hans J, Strack D. 2002. Two distantly related genes encoding 1-deoxy-D-xylulose 5-phosphate synthases: differential regulation in shoots and apocarotenoid-accumulating mycorrhizal roots. *The Plant Journal* 31:243–54
- Lois LM, Rodríguez-Concepción M, Gallego F, Campos N, Boronat A. 2000. Carotenoid biosynthesis during tomato fruit development: regulatory role of 1-deoxy-D-xylulose 5-phosphate synthase. *The Plant Journal* 22:503–13
- Kim BR, Kim SU, Chang YJ. 2005. Differential expression of three 1-deoxy-D-xylulose-5-phosphate synthase genes in rice. *Biotechnology Letters* 27:997–1001
- Cordoba E, Porta H, Arroyo A, San Román C, Medina L, et al. 2011. Functional characterization of the three genes encoding 1-deoxy-D-xylulose 5-phosphate synthase in maize. *Journal of Experimental Botany* 62:2023–38
- Phillips MA, Walter MH, Ralph SG, Dabrowska P, Luck K, et al. 2007. Functional identification and differential expression of 1-deoxy-D-xylulose 5-phosphate synthase in induced terpenoid resin formation of Norway spruce (*Picea abies*). *Plant Molecular Biology* 65:243–57
- Fan H, Wu Q, Wang X, Wu L, Cai Y, et al. 2016. Molecular cloning and expression of 1-deoxy-D-xylulose-5-phosphate synthase and 1-deoxy-D-xylulose-5-phosphate reductoisomerase in *Dendrobium officinale*. *Plant Cell, Tissue and Organ Culture* 125:381–85
- Xu Y, Liu J, Liang L, Yang X, Zhang Z, et al. 2014. Molecular cloning and characterization of three cDNAs encoding 1-deoxy-D-xylulose-5-phosphate synthase in *Aquilaria sinensis* (Lour.) Gilg. *Plant Physiology and Biochemistry* 82:133–41
- Zhang F, Liu W, Xia J, Zeng J, Xiang L, et al. 2018. Molecular characterization of the 1-deoxy-D-xylulose 5-phosphate synthase gene family in *Artemisia annua*. *Frontiers in Plant Science* 9:952
- Mandel MA, Feldmann KA, Herrera-Estrella L, Rocha-Sosa M, León P. 1996. *CLA1*, a novel gene required for chloroplast development, is highly conserved in evolution. *The Plant Journal* 9:649–58
- Wang Y, Yuan X, Li S, Chen W, Li J. 2018. Gene cloning and functional characterization of three 1-deoxy-D-xylulose 5-phosphate synthases in Simao pine. *Bioresources* 13:6370–82
- Zhang M, Li K, Zhang C, Gai J, Yu D. 2009. Identification and characterization of class 1 DXS gene encoding 1-deoxy-D-xylulose-5-phosphate synthase, the first committed enzyme of the MEP pathway from soybean. *Molecular Biology Reports* 36:879–87
- Jadaun JS, Sangwan NS, Narnoliya LK, Singh N, Bansal S, et al. 2017. Over-expression of *DXS* gene enhances terpenoidal secondary metabolite accumulation in rose-scented *geranium* and *Withania somnifera*: active involvement of plastid isoprenogenic pathway in their biosynthesis. *Physiologia Plantarum* 159:381–400
- Okada A, Shimizu T, Okada K, Kuzuyama T, Koga J, et al. 2007. Elicitor induced activation of the methylerythritol phosphate pathway toward phytoalexins biosynthesis in rice. *Plant Molecular Biology* 65:177–87
- Xi X, Zha Q, He Y, Tian Y, Jiang A. 2020. Influence of cluster thinning and girdling on aroma composition in 'Jumeigui' table grape. *Scientific Reports* 10:6877
- Mansouri H, Asrar Z, Mehrabani M. 2009. Effects of gibberellic acid on primary terpenoids and Δ^9 -tetrahydrocannabinol in *Cannabis sativa* at flowering stage. *Journal of Integrative Plant Biology* 51:553–61
- Abraham EM, Huang B, Bonos SA, Meyer WA. 2004. Evaluation of drought resistance for Texas bluegrass, Kentucky bluegrass, and their hybrids. *Crop Science* 44:1746–53
- Turgeon AJ. 1991. *Turfgrass management*. USA: Prentice-Hall Inc

26. Hooley R. 1994. Gibberellins: perception, transduction and responses. *Plant Mol Biol* 26:1529–55
27. Gan L, Di R, Chao Y, Han L, Chen X, et al. 2016. *De novo* transcriptome analysis for Kentucky Bluegrass dwarf mutants induced by space mutation. *PLoS One* 11:e0151768
28. Wright LP, Rohwer JM, Ghirardo A, Hammerbacher A, Ortiz-Alcaide M, et al. 2014. 1-Deoxyxylulose 5-phosphate synthase controls flux through the 2-C-methylerythritol 4-phosphate pathway in *Arabidopsis thaliana*. *Plant Physiology* 165:1488–504
29. Phillips MA, León P, Boronat A, Rodríguez-Concepción M. 2008. The plastidial MEP pathway: unified nomenclature and resources. *Trends in Plant Science* 13:619–23
30. Kim SM, Kuzuyama T, Chang YJ, Song KS, Kim SU. 2006. Identification of class 2 1-deoxy-D-xylulose 5-phosphate synthase and 1-deoxy-D-xylulose 5-phosphate reductoisomerase genes from *Ginkgo biloba* and their transcription in embryo culture with respect to ginkgolide biosynthesis. *Planta Medica* 72:234–40
31. Zhou W, Huang F, Li S, Wang Y, Zhou C, et al. 2016. Molecular cloning and characterization of two 1-deoxy-D-xylulose-5-phosphate synthase genes involved in tanshinone biosynthesis in *Salvia miltiorrhiza*. *Molecular Breeding* 36:124
32. Hunter WN, Bond CS, Gabrielsen M, Kemp LE. 2003. Structure and reactivity in the non-mevalonate pathway of isoprenoid biosynthesis. *Biochemical Society Transactions* 31:537–42
33. Henriquez MA, Soliman A, Li G, Hannoufa A, Ayele BT, et al. 2016. Molecular cloning, functional characterization and expression of potato (*Solanum tuberosum*) 1-deoxy-d-xylulose 5-phosphate synthase 1 (StDXS1) in response to *Phytophthora infestans*. *Plant Science* 243:71–83
34. Srinath M, Shailaja A, Bhavani B, Bindu V, Giri CC. 2017. Characterization of 1-deoxy-D-xylulose 5-phosphate synthase (DXS) protein in *Andrographis paniculata* (Burm. f.) Wall. ex. Nees: A in silico appraisal. *Ann Phytomedicine* 6:63–73
35. Yan N, Zhang H, Zhang Z, Shi J, Timko MP, et al. 2016. Organ- and growing stage-specific expression of solanesol biosynthesis genes in *Nicotiana tabacum* reveals their association with solanesol content. *Molecules* 21:1536
36. Enfissi EMA, Fraser PD, Lois LM, Boronat A, Schuch W, et al. 2005. Metabolic engineering of the mevalonate and non-mevalonate isopentenyl diphosphate-forming pathways for the production of health-promoting isoprenoids in tomato. *Plant Biotechnology Journal* 3:17–27
37. García-Alcázar M, Giménez E, Pineda B, Capel C, García-Sogo B, et al. 2017. Albino T-DNA tomato mutant reveals a key function of 1-deoxy-D-xylulose-5-phosphate synthase (DXS1) in plant development and survival. *Scientific Reports* 7:45333
38. Yang D, Ma P, Liang X, Wei Z, Liang Z, et al. 2012. PEG and ABA trigger methyl jasmonate accumulation to induce the MEP pathway and increase tanshinone production in *Salvia miltiorrhiza* hairy roots. *Physiologia Plantarum* 146:173–83
39. Estévez JM, Cantero A, Reindl A, Reichler S, León P. 2001. 1-deoxy-D-xylulose-5-phosphate synthase, a limiting enzyme for plastidic isoprenoid biosynthesis in plants. *Journal of Biological Chemistry* 276:22901–9
40. Zhang S, Ding G, He W, Liu K, Luo Y, et al. 2020. Functional characterization of the 1-deoxy-D-xylulose 5-phosphate synthase genes in *Morus notabilis*. *Frontiers in Plant Science* 11:1142
41. Kumar SR, Rai A, Bomzan DP, Kumar K, Hemmerlin A, et al. 2020. A plastid-localized *bona fide* geranylgeranyl diphosphate synthase plays a necessary role in monoterpene indole alkaloid biosynthesis in *Catharanthus roseus*. *The Plant Journal* 103:248–65
42. Gan L, Su H, Ling X, Yin S. 2017. Rust pathogen identification and mechanism of disease-resistance research on Kentucky bluegrass dwarf mutant. *Journal of Beijing Forestry University* 39:87–92
43. Sohal VK, Dey A, Singh A. 2010. MEGA biocentric software for sequence and phylogenetic analysis: a review. *International Journal of Bioinformatics Research and Applications* 6:230–40
44. Lebedeva I, Stein C. 2001. Antisense oligonucleotides: promise and reality. *Annual Review of Pharmacology and Toxicology* 41:403–19
45. Ha CD, Lemaux PG, Cho MJ. 2001. Stable transformation of a recalcitrant Kentucky bluegrass (*Poa pratensis* L.) cultivar using mature seed-derived highly regenerative tissues. *In Vitro Cellular & Developmental Biology - Plant* 37:6–11
46. Arnon DI. 1949. Copper Enzymes in Isolated Chloroplasts. Polyphenoloxidase in *Beta Vulgaris*. *Plant Physiology* 24:1–15
47. Trapnell C, Williams BA, Pertea G, Mortazavi A, Kwan G, et al. 2010. Transcript assembly and quantification by RNA-Seq reveals unannotated transcripts and isoform switching during cell differentiation. *Nature Biotechnology* 28:511–5
48. Grabherr MG, Haas BJ, Yassour M, Levin JZ, Thompson DA, et al. 2011. Full-length transcriptome assembly from RNA-Seq data without a reference genome. *Nature Biotechnology* 29:644–52



Copyright: © 2021 by the author(s). Exclusive Licensee Maximum Academic Press, Fayetteville, GA. This article is an open access article distributed under Creative Commons Attribution License (CC BY 4.0), visit <https://creativecommons.org/licenses/by/4.0/>.